Journal of Catalysis 266 (2009) 59–63

Contents lists available at ScienceDirect

Journal of Catalysis

journal homepage: www.elsevier.com/locate/jcat

Edge sites as a gate for subsurface carbon in palladium nanoparticles

Francesc Viñes [a,1], Christoph Loschen [a,2], Francesc Illas [a], Konstantin M. Neyman [a,b,*]

[a] IQTCUB & Departament de Química Física, Universitat de Barcelona, 08028 Barcelona, Spain
[b] Institució Catalana de Recerca i Estudis Avançats (ICREA), 08010 Barcelona, Spain

ARTICLE INFO

Article history:
Received 25 January 2009
Revised 29 April 2009
Accepted 13 May 2009
Available online 13 June 2009

Keywords:
Palladium catalysts
Carbonaceous deposits
Subsurface carbon
Nanoparticles
Edge sites
Activation energies
Density-functional calculations

ABSTRACT

Carbon deposits originated from side organic reactions are known to strongly affect the performance of metal catalysts. Quite unexpectedly, the C atoms have been recently found to act favorably and to lead to the enhancement of the catalyst performance. In the present work we employ a density-functional method to uncover atomistic mechanisms of the very first step of modifying Pd nanoparticles by subsurface C. In the interior of Pd(1 1 1) facets C is most stable in octahedral subsurface sites; occupation of tetrahedral subsurface sites by adsorbed C atoms results in smaller stabilization. There, the surface-to-subsurface diffusion of C features distinctive activation barriers. However, near nanoparticle edges, where CH_x decomposition precursors of C tend to be located, more mobile low-coordinated Pd atoms make the diffusion into tetrahedral subsurface sites almost non-activated. This peculiar "nano"-effect suggests that the initial low-temperature modification of Pd particles by atomic C is governed by a fast occupation of tetrahedral subsurface sites at edges, which therefore serve as a gate to the subsurface.

1. Introduction

Formation of carbonaceous deposits on metal catalysts via decomposition of reactants can strongly affect the catalytic activity and selectivity [1–4]. Recently, interest in the carbon deposition as a key event in Pd-catalyzed hydrogenation (and related) processes has drastically increased [5–8]. This has been triggered by the realized conceptual importance of carbon deposits for tailoring active sites exposed on Pd catalysts under reaction conditions. Cases of significant catalyst variation vs. the "as-prepared" one are known in heterogeneous catalysis [9]. More important is changing the old paradigm that carbon solely acts as a poison of metal catalysts through coke formation [1–3]: in fact, under certain conditions carbon can be a catalyst promoter. For instance, alkyne hydrogenation on Pd is governed by active phase Pd–C [5,6] formed in the ambient reaction conditions [10] and containing carbon atoms mainly located a few layers below the surface. It is a spectacular example that the *subsurface* area of a working catalyst cannot be neglected as it actually determines the *surface reactivity*. Decomposition of ethane [11] and acetaldehyde [12] on Pd(1 1 0) is accompanied by a similar dissolution of carbon whereas the content of carbonaceous deposits accompanying olefin hydrogenation on ordered supported Pd nanoparticles appears to be notably lower [7,8]. Nevertheless, the deposits are also thought to control the catalytic activity and selectivity. There, C atoms are hypothesized to be located in the subsurface of Pd nanoparticles [7,8] and their stabilization near edges is assumed by analogy with the methanol decomposition process [13].

Little is known at the atomic level about the very initial stage of C incorporation into Pd. Some single impurities detected on Pd(1 1 1) surface by scanning tunneling microscopy were tentatively assigned to subsurface C [14]. The assignment has been questioned in a density-functional (DF) study indicating destabilization of CO adsorption nearby the interstitial subsurface C [15], contrary to the observed CO clustering [14]. DF calculations on Pd nanoparticles [16] and a Pd(1 1 1) slab [17] classified the octahedral subsurface (*oss*) position as thermodynamically most favorable for atomic C, in line with its propensity of encapsulation in transition metal cages (e.g. [18,19]). Calculated activation barriers for the diffusion of *adsorbed* single C species from a hollow *fcc* surface site down into the *oss* position on (1 1 1) facets of the Pd_{79} nanoparticle, 60 kJ mol^{-1} [16], and on Pd(1 1 1) slab, 53 kJ mol^{-1} [17], are notably smaller than the value of 107 kJ mol^{-1} experimentally derived for high coverage of C on Pd(1 1 1) [20]. DF calculations revealed essentially no trend of atomic C adsorbed on (1 1 1) facets of Pd nanoparticles to be stabilized near the edges [21,22]. Rather, the experimentally proposed preferential location of carbonaceous deposits at edges between (1 1 1) facets of Pd

* Corresponding author. Address: IQTCUB & Departament de Química Física, Universitat de Barcelona, 08028 Barcelona, Spain. Fax: +34 93 402 1231.
E-mail address: konstantin.neyman@icrea.es (K.M. Neyman).
[1] Present address: Friedrich-Alexander-Universität Erlangen-Nürnberg, Lehrstuhl für Theoretische Chemie and Interdisciplinary Center for Interface Controlled Processes, D-91058 Erlangen, Germany.
[2] Present address: Henkel Adhesive Technologies, Scientific Computing, D-40589 Düsseldorf, Germany.

0021-9517/$ - see front matter © 2009 Elsevier Inc. All rights reserved.
doi:10.1016/j.jcat.2009.05.010

nanoparticles [13] has been rationalized by stabilization of CH_x precursors ($x \leqslant 3$) of the complete dehydrogenation products near the edges [22].

Here we perform a DF study of the very first stage of the formation of subsurface C species on ordered Pd nanoparticles. The latter have to be large enough to qualitatively represent even larger particles typical for supported model catalysts [8,13]. We examine the structure and energies of C/Pd_{140} systems with atomic C in various positions on/near (1 1 1) facets. For C at the particle edges and in the interior of the (1 1 1) facets we characterize the subsurface migration of C by the adsorption energies (E_{ads}), absorption energies (E_{abs}) in interstitial subsurface positions beneath each of the adsorption sites, and the corresponding activation energies ($\Delta E^{\neq}$). Our data reveal a very interesting "nano"-effect: the activation barrier for the subsurface diffusion of C virtually vanishes near particle edges. In combination with favored subsurface location, it suggests that the immersion of C at Pd near-edge (and similar) sites occurs rapidly already at low temperatures, whereas considerably slower subsurface diffusion from the sites on (1 1 1) terraces remote from the edges is expected. This seemingly general feature for metal nanostructures not only rationalizes the experimentally detected, almost exclusive, modification of edge and related sites of model Pd catalysts by C [13], but also opens novel means for controlling the catalytic performance.

2. Computational details and models

All DF calculations were performed with the help of the VASP code [23], an implementation of a periodic plane-wave variant of the Kohn–Sham method. The exchange-correlation (xc) functionals employed were of the local-density (LDA, VWN [24]) and generalized-gradient (GGA, PW91 [25]) types. Geometries reported in the following were optimized at the LDA level and the PW91 total energies for them were computed in a single-point fashion. This combined GGA//LDA strategy has been justified for calculations involving 4d-metal particles Pd_n [26,27] based on the observation that GGA for chemical bonds of heavy elements usually only improves energy values, but makes geometries less accurate [28]. In the absence of a "universal" xc functional equally well applicable to description of both structural and energetic parameters of Pd-containing systems under scrutiny, we have chosen to apply the GGA//LDA combination. It is computationally less demanding than the GGA//GGA scheme. Nevertheless, GGA//GGA test calculations carried out for the most critical C/Pd_{140} model (see Section 3) with atom C at the particle edge showed that GGA//LDA energies are sufficiently accurate for the purposes of the present work. In fact, comparison of PW91 energies from our test calculations for the models C/Pd_{140} (labeled as C in Fig. 2) fully optimized at the PW91 level, E_{ads} = 680 kJ mol^{-1}, E_{abs} = 709 kJ mol^{-1}, $\Delta E^{\neq}$ = 2 kJ mol^{-1}, with the corresponding PW91//VWN values, 682, 710, and ~0 kJ mol^{-1}, reveals deviations not exceeding 2 kJ mol^{-1}.

Basis sets of plane waves with kinetic energy up to 415 eV were employed. The effect of the Pd $1s^2$-$4p^6$ and C $1s^2$ core electrons on the valence electron density was accounted for via the projector augmented wave (PAW) method [29]. Geometry optimizations were performed using a conjugate gradient algorithm until forces acting on each atom became <0.03 eV/Å. A Gaussian smearing of 0.2 eV has been applied but the final energy values were extrapolated to 0 K (no-smearing). Test calculations do not reveal any noticeable spin-polarization effect for either the substrate Pd models (spin averaging resulted for Pd_{79} particle in the total energy increase by <10 kJ mol^{-1} and no distinguishable geometry change [30]) or the adsorption/absorption complexes of carbon on them (spin-polarization affected the adsorption energy of C on a Pd_{85} cluster by less than 1 kJ mol^{-1} with even smaller effect expected for the adsorption on larger particles [21]). Thus, all calculations (except for the free carbon atom reference) were non-spin-polarized.

Two complementary models of atomic C interacting with Pd were considered. (i) A six-layer Pd(1 1 1) slab with a (3×3) surface unit cell was employed to represent the interior part of large (1 1 1) facets of Pd nanoparticles. A vacuum layer of 1 nm was added in the surface direction to avoid interactions between translational replicas of the slabs. During the geometry optimization, the three uppermost layers of the Pd(1 1 1) slab were allowed to relax (together with the C species, if present), while the bottom three layers were kept fixed at the previously optimized bulk geometry. (ii) A cuboctahedral cluster Pd_{140} modeled in addition interactions of C with edge/corner sites of Pd nanoparticles. A large unit cell in this discrete system ensured a distance between replicated Pd_{140} moieties of at least 1 nm. The complete geometry relaxation of the C/Pd_{140} systems was performed. A $6 \times 6 \times 1$ Γ-centered k-point grid was used in the slab calculations. Calculations of Pd_{140} nanoparticle without or with C on it are done at the Γ point.

We define the calculated adsorption/absorption energies as $E_{ads/abs} = -E_{C/Pd} + (E_C + E_{Pd})$, where $E_{C/Pd}$ is the total energy of the adsorbed/absorbed system, E_C is the energy of the isolated C atom, and E_{Pd} is the energy of the optimized clean substrate: Pd(1 1 1) slab model or Pd_{140} nanoparticle. With this definition, stable adsorption/absorption corresponds to positive E_{ads}/E_{abs} values. Calculated formation energy of a graphene layer from single atoms C equals, at the present level of theory, 765 kJ mol^{-1} implying that this would be thermodynamically favored at a higher C coverage. However, this study is focused at the low-coverage regime, where single partially negatively charged C adatoms are present [31] and, as calculated on Pt substrates [32], their mutual repulsion helps them to stay apart from each other. Carbon diffusion subsurface (stabilizing, as shown below) should also counteract the formation of graphene.

The approximate transition states (TSs) of subsurface carbon diffusion were searched in a point-wise fashion along the path connecting adsorption and absorption configurations. For that fixed heights of the C atom over the Pd_{140} moiety were defined with respect to two most distant from C Pd layers, positions of which were kept frozen to prevent displacement of whole Pd_{140}. Subsequently, each of these approximate TSs was refined by a quasi-Newton method, in which all atomic coordinates of C/Pd_{140} cluster were included in the optimization of the nearby "zero-gradient" structure. The proper character of the minima and of the TSs were confirmed by vibrational analysis for displacements of the C atom.

3. Results and discussion

Before dealing with our data for interactions of C species with a Pd_{140} nanoparticle it is worth commenting to what extent this model represents the interactions with larger Pd nanoparticles up to the bulk limit. DF calculations on octahedral/cuboctahedral Pd clusters reveal that for the size-convergence of the adsorption energy (commonly, the most size-sensitive observable) of CO at the center of (1 1 1) facets of the nanoparticles already the cluster Pd_{79} is sufficient [26,33]; this conclusion holds for much stronger adsorbed C species as well [21]. Also, the electronic structure of the Pd_{79} model is quite similar to that of Pd bulk [30]. Thus, the even larger model cluster Pd_{140} we use here is definitely adequate for the aim of this study. Nevertheless, qualitatively insignificant differences between the interaction energies of C with surface sites in the interior of (1 1 1) facets of Pd_{140} and on the Pd(1 1 1) slab still could be noticed because the average calculated Pd–Pd bond length in Pd_{140} remains ~5 pm shorter than the Pd bulk value

[30], imposing a structural constrain in the slab calculations with three Pd layers kept frozen at the bulk geometry.

Employment of periodic boundary conditions in the present calculations provides a natural reference – slab models – for the limit of infinite surfaces. We performed calculations on a (3×3) slab modeling an extended Pd(1 1 1) surface to study subsurface diffusion of single C species at the coverage (content) $\theta_C = 1/9$ ML (monolayer) from both the *fcc* and *hcp* adsorption sites. Results are displayed in Fig. 1 (lower panel). The calculations reveal the E_{ads}, E_{abs}, and $\Delta E^{\neq}$ values in line with those of the previous PW91 slab-model calculations [17], despite slight differences in the computational procedures. Compare, e.g. our E_{abs} of C in *oss* sites, 717 kJ mol^{-1}, with the published value of 690 kJ mol^{-1} [17] or E_{ads} of C on *fcc* sites, 657 kJ mol^{-1} vs. 626 kJ mol^{-1} [17], respectively; even closer are the activation energies, for instance, for $\Delta E^{\neq}(fcc \rightarrow oss)$ 63 kJ mol^{-1} in our case vs. the literature value of 53 kJ mol^{-1} [17]. Adsorption of C in *hcp* sites of Pd(1 1 1) is very slightly, by ~5 kJ mol^{-1}, destabilized over that in *fcc* sites. (Due to the given accuracy of the DF approach, adsorption at these two sites should be considered as essentially isoenergetic). Note that in line with Ref. [17], the subsurface diffusion of the *fcc* species in the bulk direction to the corresponding tetrahedral subsurface (*tss*) site beneath it is still energetically favorable, although by as little as 6 kJ mol^{-1} only (see above). The activation barrier $\Delta E^{\neq}(hcp \rightarrow tss)$ is 15 kJ mol^{-1} lower than $\Delta E^{\neq}(fcc \rightarrow oss)$ one.

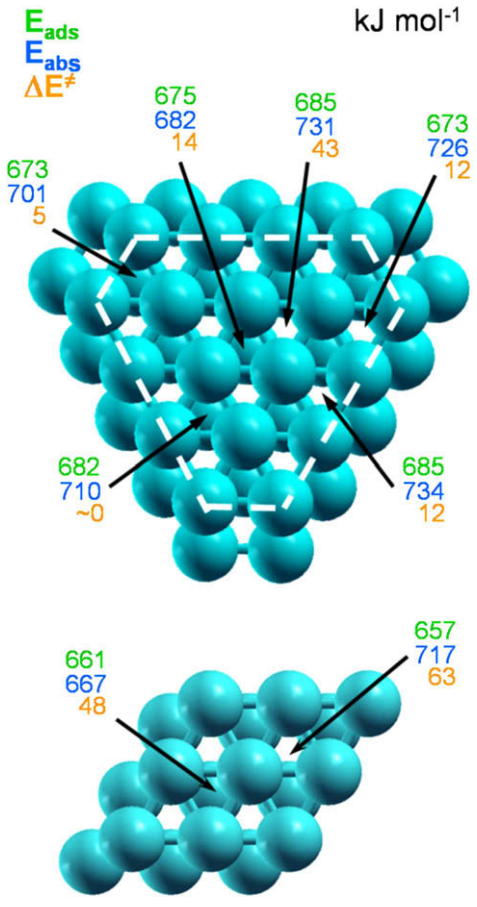

Fig. 1. Calculated energies of atomic carbon interacting with (1 1 1) facet of Pd_{140} model nanoparticle (borders of which are marked by dashed line; upper panel) and six-layer (3×3) slab Pd(1 1 1) (lower panel): adsorption energy (E_{ads}) on three-fold hollow sites, absorption energy (E_{abs}) subsurface between the first and second Pd atomic layers and the corresponding activation barriers ($\Delta E^{\neq}$) for the vertical diffusion into the subsurface octahedral and tetrahedral hollows. Only two upper Pd layers are shown for clarity. The arrows point to the surface/subsurface sites occupied by an atom C.

The just mentioned $\Delta E^{\neq}$ values computed for $\theta_C = 1/9$ ML are considerably smaller than the experimentally estimated subsurface diffusion barrier for C on single crystal Pd(1 1 1), 107 kJ mol^{-1} [20], where the steady-state surface C coverage was assumed to be close to 1 ML at a temperature around 400 K. Strongly negatively charged C species interacting with Pd [16,19] are expected to experience noticeable mutual repulsion up to long C–C distances [15,21]. This should make effects of the coverage important, similarly to DF results for C/Ni(1 1 1) revealing rather complicated influence of C content on both the interaction energies and activation barriers for subsurface diffusion [34]. We performed slab calculations at the enhanced coverage $\theta_C = 1/3$ ML using the same surface unit cell (3×3) with three C(*oss*) atoms located as far as possible from each other; for one of them vertical displacements between the sites *fcc* and *oss* are considered, [C(*oss*),C(*oss*),C($fcc \leftrightarrow oss$)]. Indeed, mainly due to the C–C repulsion, this resulted in $E_{ads}(fcc) = 635$ kJ mol^{-1} and $E_{abs}(oss) = 709$ kJ mol^{-1} decreased, respectively, by 22 and 8 kJ mol^{-1} compared to the $\theta_C = 1/9$ ML energies. Furthermore, the activation energy $\Delta E^{\neq}(fcc \rightarrow oss) = 79$ kJ mol^{-1} at $\theta_C = 1/3$ ML is 16 kJ mol^{-1} larger than that for $\theta_C = 1/9$ ML and thus closer to the experimental estimation [20]. We obtained almost quantitatively the same results for the models [C(*fcc*),C(*fcc*), C($fcc \leftrightarrow oss$)].

The E_{ads} and E_{abs} values obtained for C atoms initially located in the central *hcp* and nearby *fcc* positions on the (1 1 1) facet of the Pd_{140} particle (Fig. 1, upper panel) rather accurately reproduce our corresponding low-coverage slab-model results (Fig. 1, lower panel). Although the data obtained for C on/in the interior of the (1 1 1) facets of Pd_{140} moiety should be considered as fairly good estimates of those for extended Pd(1 1 1) surfaces, the Pd(1 1 1) slab data provide the most appropriate values to be used for examination of the interactions with sites near the particle edges to uncover "edge"-specific effects on the subsurface diffusion of C.

Carbon atoms are strongly adsorbed on *fcc* and *hcp* sites on Pd(1 1 1) facets [35]. No enhancement of the adsorption strength is found for sites near the particle edges or corners in line with previous DF studies [21]. Also, there is no particular site preference for adsorption, as revealed by small differences in the E_{ads} values, ~10 kJ mol^{-1} only, for various sites under study. A different situation emerges for absorption (subsurface C). Subsurface C is stabilized in both *oss* and *tss* sites over the respective surface sites on Pd. However, accommodation of a C atom in the more spacious *oss* site is 20–50 kJ mol^{-1} more stable than in the *tss* position. It is noteworthy that whereas the vicinity of the edge hardly stabilizes *oss* C atoms, apparent stabilization takes place for C inside *tss* sites adjacent to edges (Fig. 1). There, the E_{abs} value is enhanced by 20–30 kJ mol^{-1} with respect to the location of *tss* C at the center of the (1 1 1) facet. In the case of occupied *tss* sites, enhanced atomic mobility of such edge "defects" enables Pd nanoparticles to open and better accommodate the tensed C species.

This peculiar "nano"-effect is manifested even more evidently in the lowering of the activation barrier for subsurface diffusion of C on the sites near the edges with respect to the similar sites inside the (1 1 1) facets, more remote from the edges. Focusing on surface *fcc* and subsurface *oss* sites (see right part of Fig. 1), one can clearly recognize that a particular structural mobility of edge Pd atoms results in a stabilization of the TS with the dramatic $\Delta E^{\neq}$ drop of more than 30 kJ mol^{-1}. A similar effect is found for the barriers connecting surface *hcp* and subsurface *tss* sites (see left part of Fig. 1). Here, however, the final situation is qualitatively different: the barrier heights at edges are reduced to a few kJ mol^{-1} or almost vanish. This finding strongly suggests that *tss* sites near Pd nanoparticle edges (probably, similar to Pd surface steps) will be occupied extremely rapidly after surface atomic C is formed, despite that *tss* sites are less thermodynamically favorable than the *oss* ones. These data give a key to determine and rationalize the

scenario according to which subsurface C modifies Pd catalysts at the initial stage by preferential subsurface diffusion from sites near edges. Note that our scenario complements by adding kinetic results the very recently suggested thermodynamic picture of C interactions with planar Pd(1 1 1) and stepped Pd(211) surfaces based on slab model DF calculations [36]: taking into account C diffusion processes from surface sites near Pd steps into the subsurface, the surface step sites first occupied by C are expected to promptly release C to subsurface sites beneath them.

The enhanced flexibility of edge sites is also reflected by a trend in Pd–Pd distance alteration nearby the carbon (see Fig. 2). A comparison between *hcp*/*tss* (**A**) and *fcc*/*oss* (**B**) sites in the center of a Pd(1 1 1) facet with the corresponding sites near the particle edges (**C**,**D**) corroborates this. Note that sites **C** and **D** are more abundant on larger nanoparticles than the other two near-edge sites labeled in Fig. 1 and involving corner Pd atoms. The increased structural flexibility of the near-edge sites noticeably affects (stabilizes) only C atoms absorbed in *tss* sites (Fig. 1). It is manifested by a significant elongation of some Pd–Pd distances involved, up to 341 pm in the most stable and very flexible position **C** (Fig. 2), caused by an outward displacement of the Pd atom at the edge to accommodate subsurface C species. A similar effect is found for the TS *hcp* → *tss* and *fcc* → *oss* sites near edges. In these cases the outward movement of edge Pd atom(s) serves the purpose of creating a big enough hollow to enable C to easily diffuse subsurface. The surprisingly constant average nearest Pd–Pd distances of 314 ± 1 pm allow to considerably reduce the tension with C atoms, stabilize the TS points and concomitantly lower the $\Delta E^{\neq}$ values. These average Pd–Pd distances within the surface Pd_3 moiety near atom C are notably, by 15–30 pm, shortened in all optimized subsurface structures displayed in Fig. 2 (middle panel) except the structure C. There, the average Pd–Pd distance is elongated to 318 pm as a consequence of particularly high mobility of the edge Pd atom involved.

Finally, one should comment on the influence of adsorbed and absorbed (subsurface) atomic species C on the electronic structure of the Pd nanoparticle. The position of Pd 4d-band may serve an indicator of the surface reactivity of transition metals [37]. The calculated Pd 4d-band center of bare cluster Pd_{140} is −2.12 eV. Addition of C(*fcc*) at the edge site **D** (Fig. 2) causes a small destabilization of the 4d-band to −2.09 eV, whereas no shift of the 4d-band center is calculated for the corresponding absorption structure **D** C(*oss*)/Pd_{140}, −2.12 eV. The absence of apparent shift or its small value of 0.03 eV is related to minor overall C content of only 0.7%. In such a case local parameters may be more conclusive. To this end we probed the center of 4d density of states of three surface Pd atoms forming *fcc*/*oss* sites **D** near edge of Pd_{140} (Fig. 2). We calculated the 4d-center position for the Pd_3 moiety at −1.85 eV (Pd_{140}), −2.57 eV [C(*fcc*)/Pd_{140}], and −2.08 eV [C(*oss*)/Pd_{140}]. The downward 4d-shift could be interpreted in terms of reduced reactivity of the Pd_3 site in the presence of C; the effect is more pronounced for adsorption than for absorption, where the negative charge of C appears to be decreased. The finding that C makes nearby Pd atoms less reactive is in line with a slab model DF result that subsurface C on Pd(1 1 1) is able to notably weaken adsorption of CO molecule at a manifold of surface sites, also rather remote from the C(*oss*) [15].

Motivated by recent experiments highlighting the crucial role of subsurface carbon in various reactions catalyzed by Pd [5–8], we examined by DF calculations the initial stage of C diffusion subsurface on a large enough Pd_{140} nanoparticle in comparison with a Pd(1 1 1) surface. Those sites located at edges (or surface steps) appear to be the major gate for incorporating C atoms in interstitial subsurface sites. This is because the activation barriers almost disappear, especially at the edge *tss* sites, as mediated by more mobile Pd atoms at nanoparticle edges. These data predict the formation of a

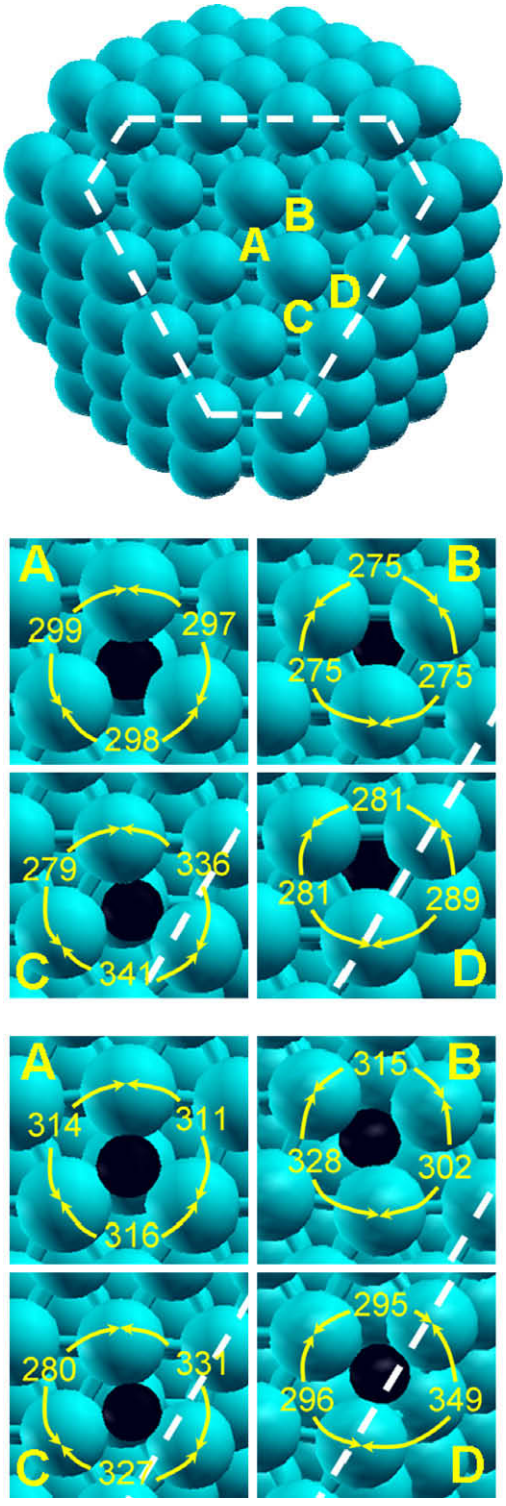

Fig. 2. Top panel: cluster model Pd_{140} with a (1 1 1) facet delimited by dashed lines. Labeled are tetrahedral **A** and octahedral **B** three-fold hollow sites in the interior of the (1 1 1) facet as well as tetrahedral **C** and octahedral **D** ones near the edge between (1 1 1) facets. Middle panel: Zoomed in view of these sites with subsurface (absorbed) carbon. Bottom panel: Zoomed in view of these sites for the transition states of the absorption process. Turquoise and black spheres represent Pd and C atoms, respectively. Selected Pd–Pd distances in pm.

Pd–C composite with C atoms in *tss* sites at Pd nanoparticle edges (or highly stepped surfaces) at very low temperatures. Raising the temperature should facilitate the emergence of *oss* C atoms at edges/steps. At even higher temperatures subsurface C is expected to also be found on extended Pd surfaces/terraces more remote from

the edges and in the interior of (1 1 1) facets of large Pd nanoparticles. There, as revealed by Pd(1 1 1) slab data, a path in which C first occupies a *tss* site and then moves to *oss* one appears to be preferred over the direct diffusion to *oss* from the surface since the two-step diffusion barriers, 48 kJ mol^{-1} (*hcp* → *tss*) and 32 kJ mol^{-1} (*tss* → *oss*) [17], are notably smaller than the direct one-step barrier *fcc* → *oss*, 63 kJ mol^{-1} obtained in the present study.

The results discussed above underline the importance of the interplay between the concentration of edge/step atoms in Pd catalysts and temperature. This information is crucial for rationalizing the broad range of experimental situations, from that when carbonaceous deposits are catalyst poisons to that when formation of subsurface C under reaction conditions is desired, e.g. to weaken adsorption of some reactants or affect hydrogen distribution, eventually leading to more reactive and selective catalysts [5–8]. The present findings should be applicable to other less expensive catalysts than Pd, such as Ni [38]. Recent DF calculations of C on Ni(1 1 1) slab showed that subsurface atomic C is thermodynamically favorable [34,39,40], with the subsurface diffusion barrier under certain conditions as high as ~180 kJ mol^{-1} [39,40]. However, as we have established above, edge sites could facilitate remarkably the subsurface penetration of C also for Ni nanoparticles in catalysts. The new experimentally evidenced chemistry of Pd catalysts modified by C together with the theoretical guidance in the preparation of such materials opens a promising way for control and improvement of metal catalysts for a broad variety of organic reactions.

4. Conclusions

Carbon deposits originated from side organic reactions are known to strongly affect the performance of metal catalysts. Quite unexpectedly, the atoms C can act favorably and *enhance* the catalyst selectivity, e.g. for partial hydrogenation of alkynes on Pd [5]. We performed density-functional calculations to uncover atomistic mechanisms of the very initial step of modifying Pd nanoparticles by subsurface C. In the interior of Pd(1 1 1) facets of Pd_{140} nanoparticle C is found to be most stable in octahedral subsurface sites; occupation of tetrahedral subsurface sites by adsorbed atoms C resulted in smaller stabilization. There, the surface-to-subsurface diffusion of C featured distinctive activation barriers. They showed a notable dependence on the coverage of carbon and calculations representing a higher-coverage situation improved agreement of the computed activation energies with the experimental estimation. The situation became qualitatively different near nanoparticle edges where CH_x decomposition precursors of C tend to be located [22]. There, more mobile low-coordinated Pd atoms at edge sites make the diffusion into tetrahedral subsurface sites almost non-activated. This peculiar "nano"-effect suggests that the initial low-temperature modification of Pd particles by atomic C is governed by a fast occupation of tetrahedral subsurface sites at edges, which therefore serve as a gate to the subsurface. These new results seem applicable also to other metal catalysts. They allow one to guide tailoring of more efficient catalysts for various industrially relevant reactions, such as selective hydrogenation, decomposition, and coupling of organic reactants and beyond.

Acknowledgments

F.V. and C.L. are grateful to Alexander von Humboldt Foundation for Postdoctoral Fellowships. F.V. also thanks the Spanish Ministry of Education and Science (MEC) for pre-doctoral Grant. Financial support was provided by the MEC (FIS2008-02238, HA2006-0102) and EU (COST-D41). Computational time on the *MARENOSTRUM* supercomputer provided by the Barcelona Supercomputing Center is gratefully acknowledged.

References

[1] Y.H. Hu, E. Ruckenstein, Adv. Catal. 48 (2004) 297.
[2] J.R. Rostrup-Nielsen, J.-H. Bak Hansen, J. Catal. 144 (1993) 38.
[3] J.H. Bitter, K. Seshan, J.A. Lercher, J. Catal. 183 (1999) 336.
[4] A. Borodziński, G.C. Bond, Catal. Rev. Sci. Eng. 48 (2006) 91, and references therein.
[5] D. Teschner, J. Borsodi, A. Wootsch, Z. Révay, M. Hävecker, A. Knop-Gericke, S.D. Jackson, R. Schlögl, Science 320 (2008) 86.
[6] D. Teschner, Z. Révay, J. Borsodi, M. Hävecker, A. Knop-Gericke, R. Schlögl, D. Milroy, S.D. Jackson, D. Torres, P. Sautet, Angew. Chem. Int. Ed. 47 (2008) 9274.
[7] B. Brandt, J.-H. Fischer, W. Ludwig, J. Libuda, F. Zaera, S. Schauermann, H.-J. Freund, J. Phys. Chem. C 112 (2008) 11408.
[8] M. Wilde, K. Fukutani, W. Ludwig, B. Brandt, J.-H. Fischer, S. Schauermann, H.-J. Freund, Angew. Chem. Int. Ed. 47 (2008) 9289.
[9] P.L. Hansen, J.B. Wagner, S. Helveg, J.R. Rostrup-Nielsen, B.S. Clausen, H. Topsøe, Science 295 (2002) 2053.
[10] D. Teschner, E. Vass, M. Hävecker, S. Zafeiratos, P. Schnörch, H. Sauer, A. Knop-Gericke, R. Schlögl, M. Chamam, A. Wootsch, A.S. Canning, J.J. Gamman, S.D. Jackson, J. McGregor, L.F. Gladden, J. Catal. 242 (2006) 26.
[11] M. Bowker, C. Morgan, N. Perkins, R. Holroyd, E. Fourre, F. Grillo, A. MacDowall, J. Phys. Chem. B 109 (2005) 2377.
[12] M. Bowker, R. Holroyd, N. Perkins, J. Bhantoo, J. Counsell, A. Carley, C. Morga, Surf. Sci. 601 (2007) 3651.
[13] S. Schauermann, J. Hoffmann, V. Johánek, J. Hartmann, J. Libuda, H.-J. Freund, Angew. Chem. Int. Ed. 41 (2002) 2532.
[14] M.K. Rose, A. Borg, T. Mitsui, D.F. Ogletree, M. Salmeron, J. Chem. Phys. 115 (2001) 10927.
[15] K.H. Lim, K.M. Neyman, N. Rösch, Chem. Phys. Lett. 432 (2006) 184.
[16] I.V. Yudanov, K.M. Neyman, N. Rösch, Phys. Chem. Chem. Phys. 6 (2004) 116.
[17] L. Gracia, M. Calatayud, J. Andrés, C. Minot, M. Salmeron, Phys. Rev. B 71 (2005) 033407.
[18] J.F. Goellner, K.M. Neyman, M. Mayer, F. Nörtemann, B.C. Gates, N. Rösch, Langmuir 16 (2000) 2736.
[19] K.M. Neyman, G.N. Vayssilov, N. Rösch, J. Organomet. Chem. 689 (2004) 4384.
[20] H. Gabasch, K. Hayek, B. Klotzer, A. Knop-Gericke, R. Schlögl, J. Phys. Chem. B 110 (2006) 4947.
[21] K.M. Neyman, C. Inntam, A.B. Gordienko, I.V. Yudanov, N. Rösch, J. Chem. Phys. 122 (2005) 174705. 1.
[22] I.V. Yudanov, A.V. Matveev, K.M. Neyman, N. Rösch, J. Am. Chem. Soc. 130 (2008) 9342.
[23] G. Kresse, J. Furthmüller, Phys. Rev. B 54 (1996) 11169.
[24] S.H. Vosko, L. Wilk, M. Nusair, Can. J. Phys. 58 (1980) 1200.
[25] J.P. Perdew, Y. Wang, Phys. Rev. B 45 (1992) 13244.
[26] I.V. Yudanov, R. Sahnoun, K.M. Neyman, N. Rösch, J. Chem. Phys. 117 (2002) 9887.
[27] F. Viñes, F. Illas, K.M. Neyman, Angew. Chem. Int. Ed. 46 (2007) 7094.
[28] A. Görling, S.B. Trickey, P. Gisdakis, N. Rösch, in: J. Brown, P. Hofmann (Eds.), Topics in Organometallic Chemistry, vol. 4, Springer, Heidelberg, 1999, p. 109.
[29] P.E. Blöchl, Phys. Rev. B 50 (1994) 17953.
[30] F. Viñes, F. Illas, K.M. Neyman, J. Phys. Chem. A 112 (2008) 8911.
[31] S.M. Davis, G.A. Somorjai, in: D.A. King, D.P. Woodruff (Eds.), The Chemical Physics of Solid Surfaces and Heterogeneous Catalysis, vol. 4, Elsevier, Amsterdam, 1983.
[32] F. Viñes, K.M. Neyman, A. Görling, J. Phys. Chem. A, submitted for publication.
[33] F. Viñes, A. Desikusumastuti, T. Staudt, A. Görling, J. Libuda, K.M. Neyman, J. Phys. Chem. C 112 (2008) 16539.
[34] J. Xu, M. Saeys, J. Phys. Chem. C 112 (2008) 9679.
[35] C adsorption and absorption in the four-fold hollow site of (001) facets, apparently less abundant on supported Pd catalysts, has also been examined. Both these initial structures spontaneously evolved in a structure where C was almost in the outermost Pd_4 plane with $E_{ads} \equiv E_{abs}$ = 745 kJ mol^{-1}.
[36] F. Studt, F. Abild-Pedersen, T. Bligaard, R.Z. Sørensen, C.H. Christensen, J.K. Nørskov, Angew. Chem. Int. Ed. 47 (2008) 9299.
[37] B. Hammer, J.K. Nørskov, Adv. Catal. 45 (2000) 71.
[38] Z. Zhang, X.E. Verykios, Catal. Today 21 (1994) 589.
[39] S.-G. Wang, X.-Y. Liao, D.-B. Cao, Y.-W. Li, J. Wang, H. Jiao, J. Phys. Chem. C 111 (2007) 10894.
[40] A. Wiltner, Ch. Linsmeier, T. Jacob, J. Chem. Phys. 129 (2008) 084704.